A genomic duplication spanning multiple P450s contributes to insecticide resistance in the dengue mosquito *Aedes aegypti*

Tiphaine Bacot[1], Chloé Haberkorn[§,1], Joseph Guilliet[§,1,2], Julien Cattel[§,1], Mary Kefi[§,3], Louis Nadalin[1], Jonathan Filee[2], Frederic Boyer[1], Thierry Gaude[1], Frederic Laporte[1], Jordan Tutagata[1], John Vontas[3,4], Isabelle Dusfour[5], Jean-Marc Bonneville[#,1], Jean-Philippe David[#,1,*]

# equal contribution
§ equal contribution
* corresponding author

[1] Laboratoire d'Ecologie Alpine (LECA, UMR 5553), Université Grenoble-Alpes (UGA), Université Savoie Mont-Blanc (USMB), CNRS, 38041 Grenoble, France.

[2] Université Paris-Saclay, CNRS, IRD, UMR Évolution, Génomes, Comportement et Écologie, 91198 Gif-sur-Yvette, France.

[3] Institute of Molecular Biology and Biotechnology, Foundation for Research and Technology Hellas, Heraklion, Greece.

[4] Pesticide Science Laboratory, Department of Crop Science, Agricultural University of Athens, Athens, Greece.

[5] Vectopôle Amazonien Emile Abonnenc, Institut Pasteur de la Guyane, Cayenne, France ; Global Health Department, Institut Pasteur, Paris, France.

* jean-philippe.david@univ-grenoble-alpes.fr

Abstract

Resistance of mosquitoes to insecticides is one example of rapid adaptation to anthropogenic selection pressures having a strong impact on human health and activities. Target-site modification and increased insecticide detoxification are the two main mechanisms underlying insecticide resistance in mosquitoes. While target-sites mutations are well characterised and often used to track resistance in the field, the genomic events associated with insecticide detoxification remain partially characterised. Recent studies evidenced the key role of gene duplications in the over-expression of detoxification enzymes and their potential use to track metabolic resistance alleles in the field. However, such genomic events remain difficult to characterise due to their complex genomic architecture and their co-occurrence with other resistance alleles. In this concern, the present work investigated the role of a large genomic duplication affecting a cluster of detoxification enzymes in conferring resistance to the pyrethroid insecticide deltamethrin in the mosquito *Aedes aegypti*.

Two isofemale lines originating from French Guiana and being deprived from major target-site mutations showed distinct insecticide resistance levels. Combining RNA-seq and whole genome pool-seq identified a 220 Kb genomic duplication spanning multiple cytochrome P450s carried by the resistant line. The genomic architecture of the duplicated loci was elucidated through long read sequencing, evidencing its transposon-mediated evolutionary origin. The importance of this P450 duplication in deltamethrin survival was supported by genotype-phenotype association and RNA interference. Experimental evolution suggested that this P450 duplication is associated with a significant fitness cost, potentially affecting its adaptive value in presence of other resistance alleles.

Overall, this study supports the importance of genomic duplications affecting detoxification enzymes in the rapid adaptation of mosquitoes to insecticides. Deciphering their genomic architecture provides new insights into the evolutionary processes underlying such rapid adaptation. Such findings and provides new tools for the surveillance and management of resistance in the field.

Key words: Mosquito; Insecticide resistance; P450; Gene duplication; Kdr mutation; *Aedes aegypti*

Introduction

Natural populations experience a wide range of selective pressures, leading to the accumulation of locally adaptive features and the expression of complex phenotypes (Orr, 2005). Among them, those driven by human activities promote novel and strong selective pressures. Understanding the genetic mechanisms allowing populations to quickly respond to rapid environmental changes has become a major goal (Hendry et al., 2008, 2017; Palumbi, 2001). Resistance of insects to insecticides is a key example of rapid evolution under strong anthropogenic selective pressures. This adaptation has occurred quickly and independently in a large number of taxa with frequent parallel trajectories (Ffrench-Constant et al., 2004; Liu, 2015). As a consequence of local and temporal variations of the selection pressures, the genetic modifications affecting resistant populations are often complex and combine several resistance mechanisms that are potentially additive, each of them bringing variable fitness costs. In addition, the very strong selection pressure exerted by insecticides is prone to produce demographic effects. Such complexity makes the identification of resistance alleles and the assessment of their respective contribution challenging (Ffrench-Constant et al., 2004; Li et al., 2007).

Besides the understanding of the genetics of rapid adaptation and the origins of complex traits, deciphering the molecular bases of insecticide resistance is also essential for improving pest management strategies (Hawkins et al., 2018). Among taxa of major economic and medical importance, mosquitoes represent a major threat for public health worldwide because of their ability to transmit human viruses and pathogens (Lounibos, 2002). Among them, *Aedes aegypti* is of particular importance because of its wide distribution and its capacity to transmit Yellow fever, Dengue, Zika and Chikungunya viruses (Brown et al., 2014). These arboviruses are now re-emerging worldwide following the expansion of mosquitoes' distribution area as a consequence of global warming, global transportation network and land perturbations (Kraemer et al., 2015). Although efforts are invested in improving vaccine-based prevention strategies (Carvalho & Long, 2021; Garg et al., 2020; Silva et al., 2018), vector control remains the cornerstone of arboviral diseases control. However, decades of insecticide usage have led to the selection and spread of insecticide resistance in this mosquito species, affecting all public health insecticides, including the most-used pyrethroids (Moyes et al., 2017). High pyrethroid resistance has been shown to reduce vector control efficacy (Dusfour et al., 2011; Marcombe, Carron, et al., 2009; Marcombe et al., 2011; Valle et al., 2019). Though greener vector control strategies are being developed, insecticides will likely remain a key component of integrated vector control in high transmission areas for the next decades (Achee et al., 2019). In this concern, identifying the genetic factors underlying resistance is crucial for tracking resistance alleles in the field and making a better use of the few authorised public health insecticides through resistance management actions (Cattel et al., 2020; Corbel & N'Guessan, 2013; Dusfour et al., 2019).

In mosquitoes, resistance to chemical insecticides is mainly caused by genetic changes decreasing the affinity of the insecticide for its target (target-site resistance), decreasing its penetration (cuticular resistance), or increasing its detoxification through complex biochemical pathways (metabolic resistance) (Li et al., 2007). Pyrethroid insecticides target the neuronal voltage-gated sodium channel (*VGSC* gene), and the selection of *knockdown resistance* (*kdr*) mutations affecting this protein can lead to resistance. Multiple *kdr* mutations, often combined as haplotypes, have been identified in *Ae. aegypti* with the following ones shown to play a key role in pyrethroid resistance: Val410Leu, Leu982Trp, Ser989Pro, Val1016Gly/Ile and Phe1534Cys (Brengues et al., 2003; Haddi et al., 2017; Hirata et al., 2014; Kasai et al., 2022; Saavedra-Rodriguez et al., 2007; Smith et al., 2016; Yanola et al., 2011). Today, these mutations can be tracked in the field using PCR-based diagnostic assays or mass sequencing approaches, providing essential information for resistance management programmes (Melo Costa et al., 2020).

Conversely, the genetic bases of metabolic resistance are far less understood, though it often accounts for a significant part of the phenotype (David et al., 2013). Indeed, the complexity and

redundancy of xenobiotic biodegradation pathways often lead to multigenic adaptations that can differ according to the nature and intensity of the selection pressure together with the demographic and ecological context (Feyereisen et al., 2015; Li et al., 2007). Metabolic resistance to pyrethroids usually results from an increased activity of detoxification enzymes such as cytochrome P450 monooxygenases (P450s or *CYPs* for genes), glutathione S-transferases (GSTs) carboxy/cholinesterases (CCEs) and UDP-glycosyl-transferases (UDPGTs) (David et al., 2013; Hemingway et al., 2004; Smith et al., 2016). At the genetic level, this can result from the selection of enzyme variants showing a higher insecticide metabolism rate, or their overexpression through cis- or trans- regulation. Genomic duplications can also contribute to overexpression, and duplications affecting detoxification genes appear frequently associated with insecticide resistance in mosquitoes (Cattel et al., 2020, 2021; Faucon et al., 2015; Weetman et al., 2018).

In addition to the genetic complexity of metabolic resistance alleles, their frequent co-occurrence with other resistance mechanisms in natural mosquito populations makes them difficult to characterise. This is the case in French Guiana, where the use of the pyrethroid deltamethrin for decades has led to the selection of highly resistant *Ae. aegypti* populations combining metabolic resistance alleles and multiple *kdr* mutations such as Val410Leu, Val1016Ile or Phe1534Cys (Dusfour et al., 2015; Haddi et al., 2017). Although the over-expression of several detoxification enzymes was supported by transcriptomics and proteomics (Dusfour et al., 2015; Epelboin et al., 2021; Faucon et al., 2017), detoxification enzymes most contributing to deltamethrin resistance and the underlying genetic events remain to be identified. A recent study using a composite population from French Guiana identified copy number variations (CNV) as a probable cause of overexpression of detoxification enzymes in this region (Cattel et al., 2020). One particular locus spanning multiple P450s showed some evidence of duplication, however the high frequency of *kdr* mutations decreased the association power while the exon-sequencing approach did not allow resolving the genomic architecture of the duplicated locus.

In this context, the present study aimed at confirming the contribution of this duplication in the resistance of *Ae. aegypti* to deltamethrin and at deciphering its genomic architecture. Two isofemale lines originating from French Guiana and showing contrasted pyrethroid resistance levels were used; both lacking two major *kdr* mutations Val1016Ile and Val410Leu occurring in South America (Epelboin et al., 2021). Controlled crosses were used to remove the Phe1534Cys *kdr* mutation from the resistant line, which retained a P450-mediated resistance phenotype. Then, RNA-seq and whole genome pool-seq confirmed the presence of a ~200 Kb genomic duplication enhancing the expression of a cluster of multiple P450 genes in the resistant line. The genomic architecture of the duplicated loci was elucidated through long read sequencing, providing clues about its evolutionary origin. Association studies, experimental evolution and reverse genetic were then used to investigate the contribution of this duplicated allele in deltamethrin resistance.

Results

Deltamethrin resistance is associated with P450 activity

Individual crossings within the resistant line IR03 allowed producing the IR0F line deprived of *kdr* mutations majorly associated with pyrethroid resistance in South America (*i.e.* Val410Leu, Val1016Ile, Phe1534Cys). However, our attempts to remove the only *kdr* mutation remaining, Ile1011Met were not successful (see below). Comparative deltamethrin bioassays showed that the IR0F line remained highly resistant to deltamethrin with 44% mortality, as compared to the IR13 line and the fully susceptible strain Bora-Bora showing 95% and 100% mortality respectively (**Table 1**). Mortality levels remains similar between the IR03 line and the IR0F line suggesting that the removal of the Phe1534Cys *kdr* mutation did not affect the resistance phenotype, or was compensated by the retaining of the Ile1011Met *kdr* mutation.

123 **Table 1. Origin, resistance status and *kdr* mutations frequencies of the studied lines**

Line	Origin, type	Deltamethrin mortality[1]	Resistance status	f(410Leu)[2,3]	f(1016Ile)[2,3]	f(1534Cys)[2,3]	f(1011Met)[3]
Bora-Bora	Fr. Polynesia, Lab	100	Susceptible	0	0	0	0
IR13	Fr. Guiana, isofemale	95 (91-99)	Low resistance	0	0	0.26	0
IR03	Fr. Guiana, isofemale	43 (26-60)	Resistant	0	0	0.26	0.33
IR0F	IR03 cross	44 (34-54)	Resistant	0	0	0	0.50

124 [1] Mortality rates (mean ±SD) previously obtained on 3 days-old females using 0.05% deltamethrin for 40 min (N=10).
125 [2] *Kdr* mutation frequencies estimated by qPCR genotyping (N=30).
126 [3] *Kdr* mutation frequencies estimated from pool-seq data.
127

128 In order to test the involvement of P450s in the pyrethroid resistance phenotype, we sequentially
129 exposed adult mosquitoes to the P450 inhibitor piperonyl butoxide (PBO) and to deltamethrin. Such
130 PBO pre-exposure did not significantly affect survival in the susceptible IR13 line, but increased
131 mortality by 20% in the IR0F line (Wilcoxon test P value = 0.009), supporting the contribution of
132 P450-mediated detoxification in the resistance of the IR0F line (**Figure 1**).

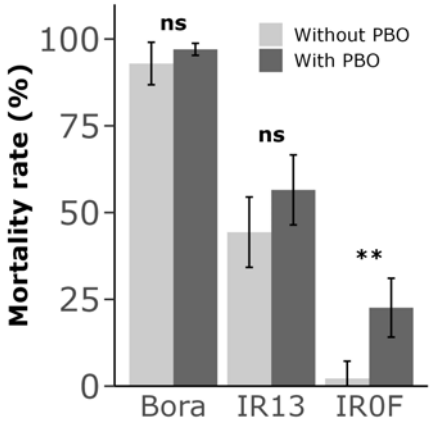

Figure 1. Synergistic effect of PBO on deltamethrin resistance. Adult females were exposed or not to 4% PBO for 1h followed by a 30-min exposure to 0.03% deltamethrin. Mortality was recorded 24h after exposure. Mean mortality rates are indicated ± SD, and compared using a Wilcoxon test (N=5, ns: not significant; **: p-value < 0.01).

143

144 *The resistance phenotype is autosomal and semi-dominant*

145 Comparative deltamethrin bioassays performed on F1 and F2 males and females from '*Bora-Bora x*
146 *IR0F'* reciprocal crosses did not support any significant bias affecting the transmission of resistance
147 alleles (**Supplementary file 1**). The mortality levels in F1 upon deltamethrin exposure were
148 intermediate to those of the parental lines for both males and females in both crosses, indicating the
149 absence of a maternal effect. Intermediate mortality levels were again observed in F2, suggesting the
150 lack of a sex transmission bias. Overall, the resistance phenotype behaved as semi-dominant.
151

152 *The resistance phenotype is associated with a duplication affecting multiple P450s*

153 RNA-seq was used to identify differentially transcribed genes between the two resistant lines (IR03
154 and IR0F), and the two susceptible lines (IR13 and Bora-Bora). Among the 11078 genes detected, 84
155 genes showed a significant and consistent differential transcription level in the four '*resistant Vs*
156 *susceptible'* pairwise comparisons (see methods, expression fold change ≥ 1.5 and adjusted P value ≤
157 0.0005). The 39 genes under-transcribed in resistant lines did not include any gene belonging to any
158 family known to be associated with insecticide resistance. Conversely, the 45 genes over-transcribed
159 in resistant lines included 8 genes belonging to gene families associated with metabolic resistance
160 (**Figure 2** and **Supplementary file 2**). These included five P450s (*CYP6BB2* AAEL014893, *CYP6-like*
161 AAEL026852, *CYP6-like* AAEL017061, *CYP6P12* AAEL014891 and *CYP9F-like* AAEL028635). The four
162 *CYP6* genes showed mean fold changes up to 4.0 folds and belong to a cluster of five consecutive

CYP6 genes located at ~271 Mb on chromosome 1. Among them, *CYP6P12* (AAEL014891) was annotated as a single accession in the reference genome while both protein sequence and RNA-seq data support the presence of two genes hereafter referred to as *CYP6P12v1* and *CYP6P12v2* when appropriate.

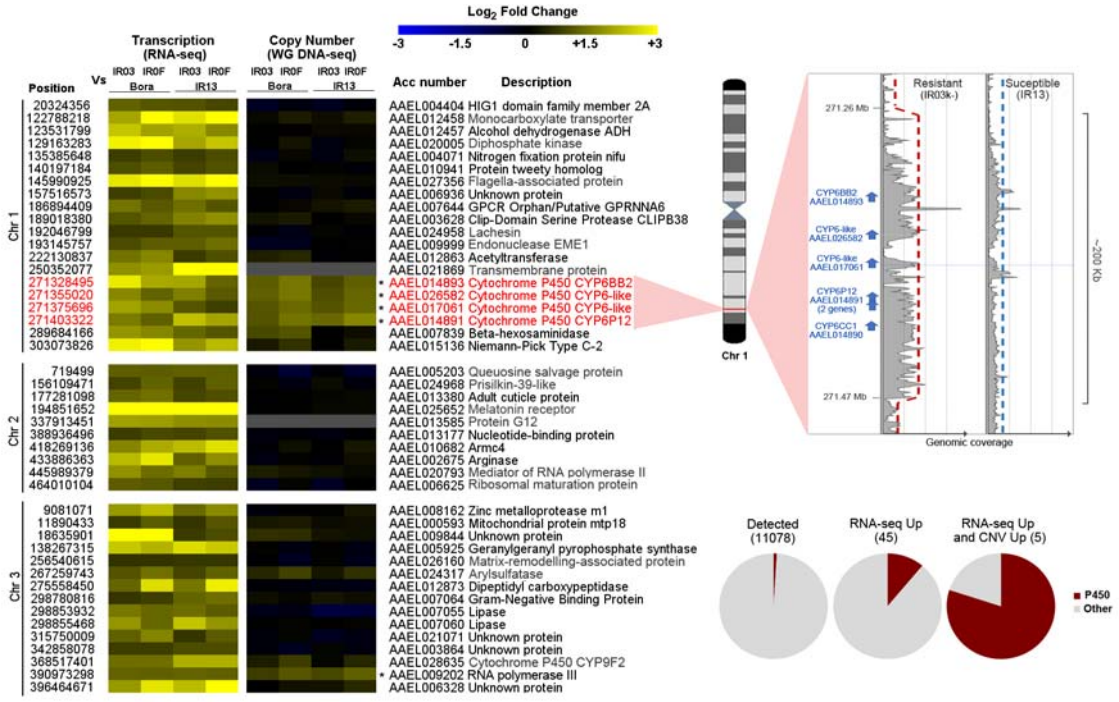

Figure 2. Genes over transcribed in resistant lines and their associated copy number variations. Only the 45 genes found significantly over transcribed from RNA-seq are shown (FC≥ 1.5 and corrected P value ≤ 0.0005 in all resistant versus susceptible pairwise comparisons). Genes also showing an elevated copy number from WG DNA-seq (FC ≥ 1.5) in all pairwise comparisons are indicated with stars. Genomic coordinates (chromosome and start position), accession number and description are indicated for all genes. Gene descriptions in grey were obtained from a BlastP against NCBI Refseq. Genes in red belong to a single duplicated region on chromosome 1. Pool-seq read coverage profiles of the susceptible IR13 and the resistant IR0F lines around the duplicated locus are shown. Pie charts show the proportion of P450s in each dataset.

Whole genome Pool-seq data were then used to identify genes affected by copy number variations in association with resistance base on their normalised exonic coverage. This analysis identified 43 genes showing congruent copy number variations between resistant and susceptible lines (FC ≥ 1.5 in all *'resistant Vs susceptible'* pairwise comparisons). The 22 genes showing an elevated copy number in resistant lines included seven P450s. One of them (AAEL009018) was located at ~58.8 Mb on chromosome 1 and was not detected as over-transcribed from RNA-seq. The six others were located at ~271 Mb on chromosome 1 and included the five *CYP6s* found over-transcribed in resistant lines (see above) and another *CYP6* (*CYP6CC1*) from the same gene cluster that was filtered out from RNA-seq analysis due to a very low transcription level (**Figure 2** and **Supplementary file 2**). A closer look at the genomic coverage at this locus revealed a ~2 folds increased coverage affecting a region of ~200 Kb spanning the entire *CYP6* cluster. Such duplication was observed in both resistant lines (IR03 and IR0F). Altogether, these genomic data suggest that the deltamethrin resistance phenotype observed in the IR03 and IR0F lines is associated with a large duplication on chromosome 1 affecting the transcription level of six clustered *CYP6* genes.

192 Whole genome pool-seq data confirmed the absence of the major Val410Leu, Val1016Ile and
193 Phe1534Cys *kdr* mutations in the resistant IR0F line, while another *kdr* mutation (Ile1011Met) was
194 identified at an exact 0.5 frequency (141/282 reads supporting the 1011Met allele). Indeed, both
195 short read and long read data revealed that this Ile1011Met mutation is part of an imperfect
196 genomic duplication covering the 21 last exons of the *VGSC* gene AAEL023266 (**Supplementary file**
197 **3**), the partial copy bearing the wild type (Ile) allele and the full-length copy bearing the resistant
198 (Met) allele (Martins et al., 2013). A 0.5 frequency thus indicates that the Ile-Met/Ile-Met genotype is
199 fixed in the IR0F line. As expected from an imperfect duplication, RNA-seq data support the sole
200 expression of the Met allele in the IR0F line, leading to a Met/Met phenotype.
201

202 *Genomic architecture of the duplication*

203 The genomic structure of the duplicated region previously identified on chromosome 1 from short
204 read data was further investigated in light of long reads data obtained from the IR13 susceptible line
205 and the IR0F resistant line. This revealed the presence of a 220.4 Kb duplication in the IR0F line, with
206 the two tandem repeats separated by a 6 Kb insertion (**Figure 3**). The right breakpoint of the
207 duplication (RB) was found ~50 Kb right to *CYP6CC1* at position 271,472,082 bp, and the left
208 breakpoint (LB) ~77 Kb left to *CYP6BB2* at 271,251,705 bp. These breakpoints were supported by split
209 reads from both long and short read data (**Supplementary file 4**). The duplication is flanked by two
210 distinct transposons, each having its own terminal inverted repeats (TIR): a 2.4 Kb PiggyBac-like
211 transposon on the right (PYL), and 9 Kb hAT-related transposon on the left (hAT-CYP6). These
212 transposons are described in more detail in **Supplementary file 5**.

213

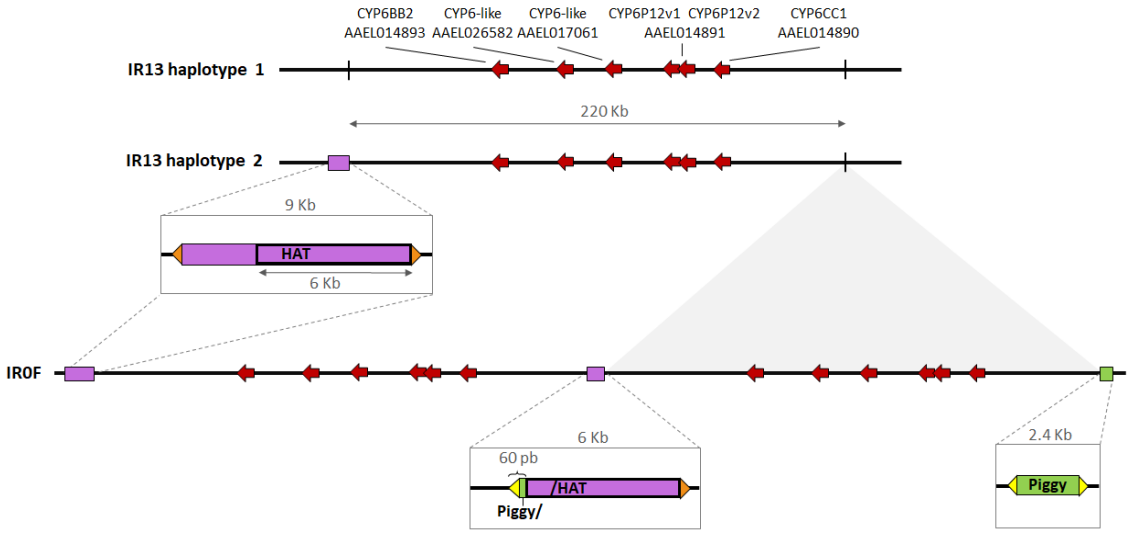

214

215 **Figure 3. Genomic architecture of the duplication.** The topology was deduced from both short and long reads sequencing
216 data. The six CYP6 genes carried by the duplication in the resistant lines are represented by red arrows. Regions containing
217 full or partial transposable elements are shown in greater detail. Orange and yellow triangles denote the inverted terminal
218 repeats from hAT (17 pb) and PiggyBac-like (18 pb) elements respectively. Diagram is not to scale.
219

220 The central sequence joining the tandem copies is chimeric, with 60 bp from the left end of PYL
221 transposon followed by 6001 bp from the right end of the hAT transposon. This duplication is absent
222 from the IR13 susceptible line (no read joining RB and LB sequences and no PYL transposon
223 sequence, neither full nor partial at RB). However, the hAT-CYP6 transposon was identified at the LB
224 in one IR13 haplotype, much like in the IR0F line, while a second haplotype was devoid of hAT
225 insertion, much like the reference genome. An excess of tri-allelic SNPs is expected within the

duplication if the two copies have diverged. To investigate this, Pool-seq data from the IR0F line were searched for such tri-allelic SNPs within the duplication and 100 Kb upward and downward. Loci were considered as tri-allelic if they carried two distinct variant alleles at the same position with a minimum allele frequency > 20%. Among the 1401 substitutions sites identified within the duplication, five were tri-allelic. No such tri-allelic variant was identified among the 1334 substitutions identified in flanking regions, representing a slight but significant enrichment in the duplicated region (Fisher test p value = 0.035). These tri-allelic sites were all located within a 11.2 Kb intergenic region between the two *CYP6-like* genes AAEL017061 and AAEL014891v1.

The P450 duplication is associated with deltamethrin survival

The association of the P450 duplication and the *kdr* Ile1011Met mutation with deltamethrin survival were investigated in F2 individuals obtained from both 'Bora-Bora x IR0F' reciprocal crosses. F2 females were then segregated with a high dose of deltamethrin (85.5% mortality) before quantifying *CYP6BB2* gene copy number and the frequency of the 1011Met *kdr* allele using ddPCR (**Figure 4**). As expected in the presence of a fixed duplication, a 2-fold increase of *CYP6BB2* copy number was observed in the IR0F line (4.31 ± 0.21 copies) as compared to Bora-Bora line (2.07 ± 0.10 copies) while F1 individuals showed an intermediate copy number (3.58 ± 0.14 copies). In deltamethrin segregated F2 individuals, *CYP6BB2* copy number was higher in survivors than in dead individuals (4.00 ± 0.16 copies versus 3.31 ± 0.15 copies) supporting a genetic linkage between the P450 duplication and resistance. Resistance was also linked to the *kdr* mutation Ile1011Met on chromosome 3. In line with an heterogenous *kdr* duplication, the frequency of the Met allele was close to 0.5 in the IR0F resistant line and close to 0.33 in F1 individuals. In deltamethrin-segregated F2 individuals, the Met allele frequency was higher in survivors than in dead individuals (0.41 ± 0.02 versus 0.30 ± 0.02).

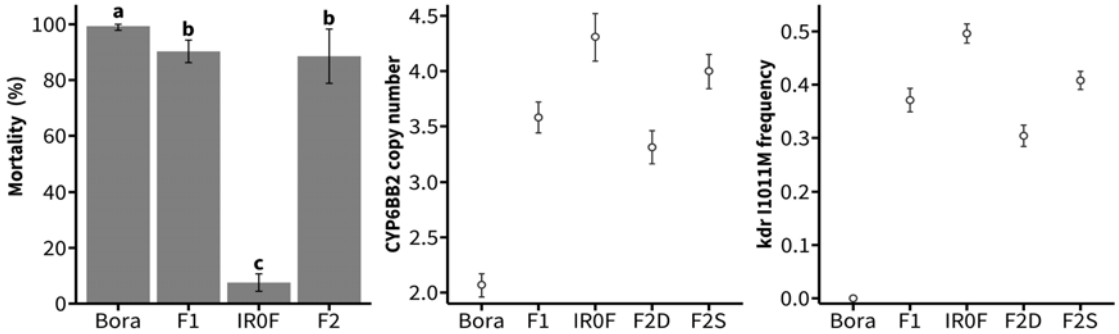

Figure 4. Genotype-phenotype association study. Genotype-phenotype association study. Left panel shows mortality data obtained by exposing adult females from the IR0F and Bora-Bora lines and their F1 and F2 progeny to 0.03% deltamethrin for 1 hour. Mean mortalities ± SD 24h after insecticide exposure are shown and distinct letters indicate significant mortality differences (significant Kruskal-Wallis test followed by post hoc Wilcoxon test with Bonferroni-Holm correction, N ≥ 5, p ≤ 0.05). Middle and right panels show the copy number of *CYP6BB2* and the frequency of the *kdr* 1011Met allele respectively as inferred by ddPCR on pools of individuals (mean ± 95% CI, Bora: N=19, IR0F: N=23, F1: N=17, F2D: N=113, F2S: N=15). Dead and surviving F2 individuals 24h after insecticide exposure are noted F2D and F2S respectively.

Multiple P450s carried by the duplication may contribute to deltamethrin survival

The relative importance of the P450s carried by the duplication in deltamethrin survival was then examined by RNA interference. Direct dsRNA injections in adult females of the IR0F line were used to specifically knock down the five *CYP6* genes showing sufficient expression to be detected by RNA-seq (*CYP6BB2*, *CYP6-like* AAEL026582, *CYP6-like* AAEL017061, *CYP6P12v1* and *CYP6P12v2*). Such approach allowed reaching an acceptable silencing specificity and a moderate silencing efficiency (from 42.2% for AAEL017061 to 69.7% for AAEL026582). Comparative deltamethrin bioassays

266 performed on dsCYP6-injected mosquitoes and dsGFP-injected controls suggested that the two first
267 CYP gene of the duplicated cluster (*CYP6BB2* and *CYP6-like* AAEL026582) contribute to deltamethrin
268 survival (see methods and results in **Supplementary file 6**). However, data generated across multiple
269 injection experiments were not fully conclusive because a high mortality was frequently observed in
270 dsGFP-injected controls and because the increased mortality observed in dsCYP-injected mosquitoes
271 were relatively low probably due to the moderate silencing efficiency and the presence of the *kdr*
272 1011Met allele in the IR0F line.
273

274 *The duplication is hardly retained by selection in presence of the 1011Met kdr allele*

275 The co-occurence of the P450 duplication and the Ile1011Met *kdr* mutation in the IR0F resistant line
276 was taken as an opportunity to compare their responses to deltamethrin selection. Four independent
277 lines obtained from 'Bora-Bora x IR0F' F3 offspring and representing two replicated selection regimes
278 (selected lines: SelA and SelB, non-selected lines: NSA and NSB) were compared for their resistance
279 level, *CYP6BB2* copy number and *kdr* 1011Met allele frequency (**Figure 5**).

280

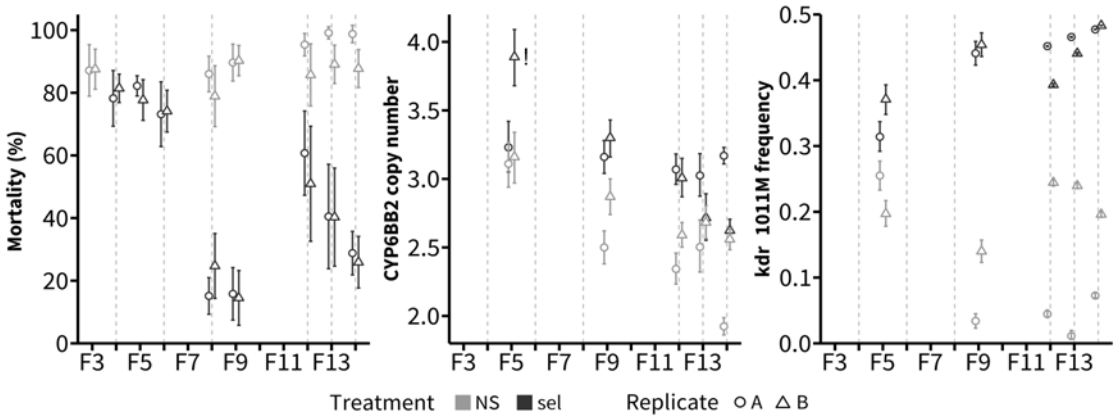

281

282 **Figure 5: Response of the P450 duplication and the *kdr* 1011Met allele to deltamethrin selection.** Experimental evolution
283 was performed from the F3 offspring of 'Bora-Bora x IR0F' reciprocal cross using two replicate lines for each selection
284 regime: deltamethrin-selection (SelA and SelB lines, black) and no selection (NSA and NSB lines, grey). Circles and triangles
285 distinguish replicates A and B. Grey dashed lines indicate the generations for which Sel lines were selected with
286 deltamethrin. Left panel shows the resistance of each line as measured by bioassays with 0.03% deltamethrin (mean
287 mortality ± SD). Middle and right panels show the copy number of CYP6BB2 and the frequency of the kdr 1011Met allele
288 respectively as inferred by ddPCR on pools of individuals (mean ± 95% CI, N ≥ 30). The SelB *CYP6BB2* copy number data
289 point marked with a '!' was caused by an unexpected sampling bias and was therefore not included in the statistical analysis
290 comparing *CYP6BB2* copy number between Sel and NS lines across generation (Linear Mixed Effect Model, p=0.0088).

291

292 An increase of deltamethrin resistance was observed for both Sel lines, with mortality dropping from
293 ~80% in F4 to less than 20% in F9. Relaxing deltamethrin selection for three successive generations
294 (F9 to F11) lead to an increased mortality in both Sel lines, suggesting that the resistance phenotype
295 is costly. Though subjected to sampling effects, ddPCR data showed that the *kdr* 1011Met allele was
296 rapidly selected by deltamethrin. Its frequency was close to 0.5 in F9 of both Sel lines, supporting the
297 near fixation of the Ile-Met duplicated allele. Such increased frequency was not seen in NS lines
298 where Met allele frequency decreased to less than 10% in one line and fluctuated under 0.25 in the
299 other line. No such strong response to selection was observed for the P450 duplication, with
300 *CYP6BB2* copy number showing a gradual decrease through generations in both Sel and NS lines.
301 However, *CYP6BB2* mean copy number were significantly higher in Sel lines than in NS lines across
302 generations, supporting a higher retention rate of the duplicated allele upon deltamethrin selection
303 (Linear Mixed Effect Model, p value = 0.0088).

304

305 # Discussion

306 In line with their high probability of occurrence, genomic duplications have been shown to frequently
307 contribute to short-term adaptation in various organisms (Kondrashov, 2012). In arthropods facing
308 strong selection pressures from insecticides, duplications are known to be adaptive via two distinct
309 mechanisms (Bass & Field, 2011). First, heterogeneous duplications affecting key insecticide target
310 genes and tethering both susceptible and resistant alleles have been associated with a reduction of
311 fitness costs (Labbe et al., 2007). Second, duplications of detoxification genes can contribute
312 quantitatively to their over-expression, leading to resistance through increased insecticide
313 metabolism (Faucon et al., 2015; Weetman et al., 2018). As opposed to target-site resistance
314 mutations that can be easily tracked by PCR in natural populations, the paucity of DNA markers
315 underlying metabolic resistance hinders their tracking in the field. In this concern, identifying gene
316 duplications associated with metabolic resistance can provide new tools to monitor the dynamics of
317 resistance alleles (Cattel et al., 2021).
318

319 *A genomic duplication affects a cluster of P450s previously associated with resistance*

320 The present study confirmed the occurrence of a large genomic duplication affecting a cluster of six
321 P450s from the *CYP6* family in *Ae. aegypti* populations from French Guiana. The presence of such a
322 duplication was previously suspected though the structure of the duplicated loci could not be
323 resolved from targeted-sequencing data (Faucon et al., 2015). The association of this P450
324 duplication with deltamethrin resistance was supported by controlled crosses, although the presence
325 of other resistance alleles limited the association power (Cattel et al., 2020). A duplication
326 encompassing the *CYP6BB2* gene was also associated with pyrethroid resistance in Lao PDR
327 (Marcombe et al., 2019), suggesting a wider geographic distribution. Though gene duplication was
328 not looked for, the over-transcription of CYP6 genes from this cluster (e.g. *CYP6BB2*, *CYP6P12* and
329 *CYP6CC1*) was frequently associated with pyrethroid resistance worldwide (Bariami et al., 2012;
330 Dusfour et al., 2015; Goindin et al., 2017; Kasai et al., 2014; Marcombe, Poupardin, et al., 2009;
331 Moyes et al., 2017; Reid et al., 2014; Saavedra-Rodriguez et al., 2012; Seixas et al., 2017). These
332 genes were also found under directional selection in association with pyrethroid survival in a
333 Mexican resistant line from whole exome SNP data (Saavedra-Rodriguez et al., 2021). In addition,
334 *CYP6BB2* was also shown capable of metabolising the pyrethroid permethrin (Kasai et al., 2014). By
335 comparing its copy number and transcriptional level across different lines, Faucon et al. (2017)
336 suggested that both transcriptional regulation and genomic duplication contribute to its over-
337 expression in South America. Interestingly, this gene also responded to selection with the
338 neonicotinoid imidacloprid, suggesting that P450s from this cluster can be selected by and
339 metabolise other insecticides (Riaz et al., 2013; Zoh et al., 2021).

340 Our attempt to isolate this P450 duplication from other resistance alleles occurring in French Guiana
341 was partially successful. Indeed, both isofemale lines were naturally deprived from the major
342 Val1016Iso and Val410Leu *kdr* mutations, and controlled crosses allowed removing the Phe1534Cys
343 mutation. However, the resulting IR0F resistant line carrying the P450 duplication still carried the
344 Ile1011Met *kdr* mutation as a fixed heterogenous duplication (Ile-Met/Ile-Met genotype, Met/Met
345 phenotype). Nevertheless, the use of the P450 inhibitor PBO showed that the resistance phenotype
346 was still associated with P450-mediated metabolism. Considering that four of the five P450s over-
347 transcribed in resistant lines belong to the duplicated loci, their contribution to the resistance
348 phenotype is likely. Studying the mode of transmission of resistance did not allow evidencing any
349 significant maternal effect or sexual transmission bias potentially associated with resistance. In line
350 with this, this P450 duplication is located outside of a 210 Mb region of chromosome 1 showing a low

351 recombination rate and a high genetic differentiation between *Ae. aegypti* males and females
352 (Fontaine et al., 2017).
353

354 *The architecture of the P450 duplication suggests a recent ectopic recombination event*

355 The presence of two distinct transposons at the duplication breakpoints that they have played an
356 active role in the generation of this genomic event. Transposon-mediated duplication often arises
357 from ectopic recombination between two homologous transposon copies inserted in the same
358 orientation at distinct positions of a same chromosome (Baker et al., 1996). However, such an event
359 would leave a single full-length transposon copy between the two duplicated genomic regions with
360 no transposon at other breakpoints (Remnant et al., 2013). Here, a more complex scenario must
361 have taken place because two distinct transposons are flanking the duplication, and because the
362 sequence joining the two copies is chimeric. A possible scenario involves independent insertion of
363 the two distinct transposons, then transposition of the hAT into the PiggyBac-like transposon
364 followed by a deletion event, and finally an ectopic homologous recombination event between the
365 two duplicated hAT sequences (**Supplementary File 7**). One transposon involved is related to the hAT
366 superfamily while the other one is distantly related to PiggyBac (see **Supplementary file 5** for more
367 details), both being cut and paste elements having multiple copies and being active in the *Ae. aegypti*
368 genome (Nene et al., 2007). The divergence of the two tandem copies was supported by the
369 identification of a few tri-allelic substitution sites within the duplicated region. Though the frequency
370 of such tri-allelic sites is likely underestimated (*i.e.* reverting mutations to the wildtype allele not
371 detected as tri-allelic), such low divergence supports the recent age of this duplication event.
372

373 *The P450 duplication is associated with deltamethrin survival but its adaptive value may be*
374 *balanced by its fitness cost*

375 The association study confirmed the association of the P450 duplication with deltamethrin survival
376 together with the Ile1011Met *kdr* mutation. As the *VGSC* gene carrying *kdr* mutations is located on
377 chromosome 3, a genetic linkage between these two loci is excluded. The association of the P450
378 duplication in F2, following limited recombination events, implies a resistance locus located on
379 chromosome 1, either the P450 duplication itself or another genetically linked locus. However, no
380 other known resistance gene was identified in this genomic region in the present study. The
381 association of the Ile1011Met *kdr* mutation with deltamethrin survival was expected. Indeed,
382 although less efficient than other *kdr* mutations (Brito et al., 2018), there is evidence that this
383 mutation confers some resistance to deltamethrin in the field (Brengues et al., 2003; Martins et al.,
384 2009). As previously suggested, we identified that this *kdr* mutation is part of a heterogenous
385 duplication (Martins et al., 2013). Our RNA-seq data supported the sole expression of the Met allele
386 in the IR0F resistant line, suggesting that the wild type Ile allele is carried by a pseudo gene.

387 The relative importance of the different *CYP6* genes carried by the P450 duplication in deltamethrin
388 survival was investigated through RNA interference. Despite a limited statistical power, likely due to
389 the presence of the *kdr* Ile1011Met resistance allele and moderate knock down efficiencies, these
390 data suggest that at least two *CYP6* genes (*CYP6BB2* and AAEL026582) carried by the duplication may
391 contribute to deltamethrin survival.

392 Experimental evolution confirmed the strong positive response of the *kdr* 1011Met allele to selection
393 with a high dose of deltamethrin. Such experiment also evidenced a gradual decrease of this allele in
394 both non-selected lines, supporting a fitness costs in absence of insecticide as previously shown for
395 other *kdr* mutations (Rigby et al., 2020; Uemura et al., 2023). Indeed, the co-existence of the Met
396 allele carried by the full length *VGSC* gene and the duplicated Ile allele carried by a pseudogene
397 would not confer a fitness cost reduction as seen for the Ace-1 locus in *Culex pipiens sp.* and
398 *Anopheles gambiae* where both alleles contribute to the phenotype (Djogbenou et al., 2009; Labbe

et al., 2007). In this regard, further investigating the evolutionary origin and dynamics of this *kdr* duplication in relation to insecticide selection pressure deserves further attention.

The association of the P450 duplication with resistance was less clear. A gradual decrease of *CYP6BB2* copy number was observed in both selected and non-selected lines, even though such decay was slower in the selected lines. Such result may indicate the presence of a significant fitness cost associated with this large genomic duplication, that is not compensated by its adaptive value in our laboratory conditions. Indeed, genomic duplications can be detrimental for various reasons (Schrider et al., 2013): first, gene duplications can alter the gene dosage balance which can lead to metabolic cost. Second, genomic duplications allow the accumulation of deleterious mutations that are less cleared off by background selection because of the functional redundancy of duplicated copies. Third, large duplications can impair recombination locally. In the present case, a low recombination rate at this locus between the Bora-Bora line (well adapted to laboratory conditions) and the IR0F line (less fitted to our laboratory conditions) may have impaired the selection of the P450 duplication and favoured the selection of the *kdr* 1011Met allele. Finally, considering the fitness costs associated with this *kdr* mutation, its additive cost with the P450 duplication may have prevented their concomitant selection with the use of high insecticide dose favouring the selection of the former. Such fitness-cost balance at two distinct loci may reflect the complex interactions occurring between resistance alleles *in natura*, leading to distinct adaptive trajectories depending on selection pressures and demographic effects.

Conclusions

Following previous work, the present study supports the contribution of this P450 duplication in pyrethroid resistance. However, deciphering its adaptive value *versus* other resistance alleles and its dynamics in natural mosquito populations deserves further work. The relative importance of the different *CYP6* genes carried by this duplication in resistance to pyrethroids (and possibly to other insecticides) also deserves further validation. Despite this incomplete picture, the nature of the P450s affected by this large genomic duplication and their frequent association with insecticide resistance call for further studying its evolutionary origin and dynamics in response to xenobiotics. In this context, though the flanking of the duplication by repeated transposable elements prevented the design of a specific PCR diagnostic assay targeting the breakpoints, the dual-colour quantitative TaqMan ddPCR assay we developed (see **Supplementary file 8**) represents a good alternative to track this resistance allele in natural mosquito populations.

Methods

Mosquitoes

The *Ae. aegypti* laboratory strain Bora-Bora, fully susceptible to insecticides was used as reference in the present study. The isofemale lines used in the present study were derived from a field population collected in 2015 in the Ile Royale (IR) island (5.287° N; 52.590° W) off the coast of French Guiana as described in Epelboin et al. (2021). Among the isofemale lines isolated from this population, the lines IR13 and IR03 showed contrasted pyrethroid resistance levels with the IR03 line being highly resistant and the IR13 line being susceptible. Both lines were shown to lack the two major voltage-gated sodium channel *kdr* mutations occurring in this geographical area (Val410Leu and Val1016Ile), yet both carried the Phe1534Cys mutation at a moderate frequency (Epelboin et al., 2021). The proteomic profiling of these lines identified multiple cytochrome P450s enriched in the IR03 resistant line as compared to a susceptible line, supporting the presence of metabolic resistance alleles (Epelboin et al., 2021). All mosquito lines were maintained under standard laboratory conditions (27 ± 2°C, 70 ± 10 % relative humidity, light/dark cycle 14:10h) and large population size to limit drift

446 effects (N>1000). Larvae were reared in tap water and fed with hay pellets. Adults were maintained
447 in mesh cages and fed with a 10% honey solution. Blood feedings were performed on mice.
448

449 *Removal of the Phe1534Cys mutation from the IR03 line*

450 In an attempt to isolate metabolic resistance alleles, inter-crosses assisted by genotyping were
451 performed on the IR03 resistant line to create the IR0F line depleted from the Phe1534Cys *kdr*
452 mutation. A total of 245 IR03 couples were individualised at the pupal stage in eppendorf tubes
453 placed in plastic cups covered by a nylon mesh and allowed to emerge and reproduce. The
454 Phe1534Cys Kdr mutation was first searched for from male exuvia for all couples and then from
455 female exuvia of the 58 couples from which males were negatives for the 1534Cys allele. Genotyping
456 was performed on qPCR using the High Resolution Melt Curve Analysis method as described in
457 Saavedra-Rodriguez et al. (2007). The six couples in which both parents were homozygous wild type
458 (Phe-Phe) were transferred to a mesh cage, blood fed and allowed to lay eggs. The absence of the
459 1534Cys allele in the offspring was confirmed by genotyping 40 individuals of both sexes. Adults were
460 then exposed to 0.05% deltamethrin and survivors were allowed to freely reproduce to generate the
461 IR0F resistant line. The IR0F line was then maintained in standard insectary conditions under
462 moderate deltamethrin selection pressure (*i.e.* 50% mortality every two generations).
463

464 *Deltamethrin bioassays*

465 All bioassays were performed by exposing replicates of 20-25 three days-old non-blood-fed adults to
466 deltamethrin impregnated filter papers following the standard WHO procedure, with mortality being
467 recorded 24h after insecticide exposure (WHO, 2022). Different doses and exposure times were used
468 according to the nature of the mosquito tested (susceptibility status, sex, use of enzymatic inhibitor)
469 in order to maximise the mortality variations observed. Bioassay assessing the resistance level of the
470 different lines was performed on females using 10 replicates per line and a dose of 0.05%
471 deltamethrin for 40 min. The involvement of P450s in the resistance phenotype was assessed by
472 comparing deltamethrin mortality of females exposed or not to filter papers impregnated with 4%
473 piperonyl butoxide (PBO) for 1h prior to deltamethrin bioassay. This bioassay was performed on 5
474 replicates for each condition and a dose of 0.03% deltamethrin for 30 min. In order to investigate the
475 mode of inheritance of resistance, comparative bioassays were performed on males and females
476 obtained from the susceptible Bora-Bora line and the resistant IR0F line together with F1 and F2
477 individuals obtained from their reciprocal crosses (see below). Deltamethrin exposure conditions
478 were 0.03% deltamethrin for 30 min for females and 0.015% deltamethrin for 25 min for the males
479 to account for their inherent lower insecticide tolerance. Bioassays used for monitoring the
480 resistance level of the selected and non-selected lines during experimental evolution were
481 performed on 5 to 7 replicates per line per generation using a dose of 0.03% deltamethrin for 1h.
482

483 *Controlled cross and association studies*

484 In order to investigate the mode of inheritance of resistance, reciprocal crosses between the fully
485 susceptible Bora-Bora line and the resistant IR0F line were performed (cross A: 'Bora-Bora females x
486 IR0F males' and cross B: 'IR0F females x Bora-Bora males'). Crosses were performed with 200 virgin
487 females and males of each line. The susceptibility of F1 and F2 males and females from each cross
488 were then compared using deltamethrin bioassays as described above. The association of the P450
489 duplication with deltamethrin survival was studied in F2 females obtained from both reciprocal
490 crosses. Females were segregated with 0.03% deltamethrin for 1h leading to 88.5% mortality after a
491 24h recovery time. Dead and alive females were sampled and stored at -20°C until molecular
492 analyses. The response of the P450 duplication and the Ile1011Met *kdr* mutation were further
493 studied across multiple generations using experimental selection. F3 eggs obtained from the two
494 reciprocal crosses A and B were pooled in equal quantity and then randomly split in 4 lines: the first

495 two lines (NSA and NSB) were maintained without insecticide selection, while the two other lines
496 (SelA and SelB) were selected with deltamethrin. This duplicated line setup was used in order to
497 control for genetic drift that may occur across generations. Deltamethrin mass selection was
498 performed prior mating on both virgin males and virgin females (N>1000 for each line) at generations
499 F4, F6, F8, F12 and F13. A constant dose of deltamethrin was used through the selection process
500 leading to ~70% mortality in each sex at generation F3 (females: 0.03% for 1h; males: 0.015% for 30
501 min). The resistance level of each line was monitored at generations F5, F9, F12, F13 and F14 on
502 females prior to insecticide selection using standard bioassays (see above). Unexposed adult females
503 from each line were sampled at the same generations and stored at -20°C until molecular analysis.
504

505 *RNA-sequencing*

506 Gene transcription levels were compared across the four lines (Bora-Bora, IR13, IR03 and IR0F) using
507 RNA-seq. For each line, four RNA-seq libraries were prepared from distinct batches of 25 calibrated
508 three-day-old non-blood-fed females not exposed to insecticide. Total RNA was extracted using
509 TRIzol (Thermo Fisher Scientific) following manufacturer's instructions. RNA samples were then
510 treated with RNase-free DNase set (Qiagen) to remove gDNA contamination, purified on RNeasy mini
511 columns (Qiagen) and QC checked using Qubit (Thermo Fisher Scientific) and bioanalyzer (Agilent).
512 RNA-seq libraries were prepared from 500 ng total RNA using the NEBNext® Ultra™ II directional RNA
513 library Prep Kit for Illumina (New England Biolabs) following manufacturer's instructions. Briefly,
514 mRNAs were captured using oligodT magnetic beads and fragmented before being reverse
515 transcribed using random primers. Double-stranded cDNAs were synthesised, end-repaired, and
516 adaptors were incorporated at both ends. Libraries were then amplified by PCR for 10 cycles and
517 purified before QC check using Qubit and Bioanalyzer. Libraries were then sequenced in multiplex as
518 single 75 bp reads using a NextSeq500 sequencer (Illumina). An average of 51.4 M reads was
519 generated per library. After unplexing and removing adaptors, sequenced reads from each library
520 were loaded into Strand NGS V3.2 (Strand Life Science) and mapped to the latest *Ae. aegypti* genome
521 assembly (Aaeg L5) using the following parameters: min identity = 90%, max gaps = 5%, min aligned
522 read length = 25, ignore reads with > 5 matches, 3 end read trimming if quality < 20, mismatch
523 penalty = 4, gap opening penalty = 6, gap extension penalty = 1. Mapped reads were then filtered
524 based on their quality and alignment score as follows: mean read quality > 25, max N allowed per
525 read = 5, alignment score ≥ 90, mapping quality ≥ 120, no multiple match allowed, read length ≥ 35.
526 These filtering steps allowed retaining ~75% of reads. Quantification of transcription levels was
527 performed on the 13614 protein-coding genes using the DESeq2 method with 1000 iterations
528 (Anders & Huber, 2010, https://bioconductor.org/packages/release/bioc/html/DESeq2.html). Only
529 the 11449 genes showing a normalised expression level ≥ 0.5 (~0.05 RPKM) in all replicates for all
530 lines were retained for further analysis. Differential gene transcription levels between each line
531 across all replicates were then computed using a one-way ANOVA followed by a Tukey post hoc test
532 and p values were corrected using the Benjamini and Hochberg multiple testing correction
533 (Benjamini & Hochberg, 1995). Genes showing a transcription variation ≥ 1.5 fold (in either direction)
534 and an adjusted p value ≤ 0.0005 in the four pairwise comparisons between resistant and susceptible
535 lines (*i.e.* IR03 Vs Bora-Bora, IR03 Vs IR13, IR0F Vs Bora-Bora and IR0F Vs IR13), were considered
536 differentially transcribed in association with deltamethrin resistance.
537

538 *Whole genome Pool-seq and CNV analysis*

539 The genome of the four lines were compared using whole genome pool-seq. For each line, genomic
540 DNA was extracted from two batches of 50 adult females using the PureGene Core Kit A (Qiagen) and
541 the two gDNA extracts were then pooled in equal proportion into a single sequencing library. Whole
542 genome sequencing was performed from 200 ng gDNA. Sequencing libraries were prepared
543 according to the TruSeq DNA Nano Reference guide for Illumina Paired-end Indexed sequencing
544 (version oct. 2017) with an insert size of 550 bp. Sequencing was performed on a NextSeq 550

545 (Illumina) as 150 bp paired-reads. Sequencing depth was adjusted to reach an average coverage ≥
546 80X leading to the sequencing of ~713 M reads per library. Reads obtained from each line were
547 loaded into Strand NGS V3.2 and mapped to *Ae. aegypti* genome (Aaeg L5) using the following
548 parameters: min identity = 90%, max gaps = 5%, min aligned read length = 25, ignore reads with > 5
549 matches, 3 end read trimming if quality < 15, mismatch penalty = 4, gap opening penalty = 6, gap
550 extension penalty = 1. Mapped reads were then filtered based on their quality and alignment score
551 as follows: mean read quality > 25, max N allowed per read = 5, alignment score ≥ 90, mapping
552 quality ≥ 60, no multiple match allowed, read length ≥ 100. Finally, interchromosomal split reads and
553 PCR duplicates were removed. These filtering steps allowed retaining ~53% of reads. In order to
554 focus on duplication impacting protein expression, gene copy number variation (CNV) analysis was
555 performed on exons of all protein-coding genes. For each gene, raw coverages were obtained by
556 dividing the number of reads mapped to all (non-overlapping) exons by total exon length. Normalised
557 gene coverages were then obtained by dividing raw gene coverages by the total number of reads
558 passing mapping and quality filters from each sequenced library. In order to limit false positives in
559 low coverage regions, genes showing a normalised coverage value < 1E-8 in at least one line were
560 filtered out (12145 genes retained). As for RNA-seq, genes showing a CNV ≥ 1.5 fold (in either
561 direction) in the four pairwise 'resistant *vs* susceptible' comparisons were considered affected by
562 CNV in association with resistance.
563

564 *Long read sequencing and de novo assembly of the P450 duplication*

565 The genomic architecture of the duplicated locus was further examined in the duplicated IR0F line
566 versus the non-duplicated IR13 line. Both lines were submitted to long read sequencing using oxford
567 nanopore technology. Genomic DNA was extracted from pools of 75 adult females using the Gentra
568 Puregene Tissue kit (Qiagen) with 3 mL cell lysis buffer. Genomic DNA was quantified using Qubit
569 DNA Broad Range assay (Qiagen) and quality-checked by agarose gel electrophoresis before adjusting
570 concentration to 150 ng/µl. High genomic DNA fragments were selected using the Short Read
571 Eliminator kit (Circulomics). DNA libraries were prepared using 1 µg gDNA with the ligation
572 sequencing kit SQK-LSK109 kit (Oxford Nanopore) following manufacturer's instructions. Finally, 50
573 fmoles of the resulting DNA library were loaded on a R9.4.1 MinIon flow cell. Long read sequences
574 were collected from 2 independent runs of 48 h for each line. Sequencing generated a total of
575 515K/1017K reads with an average length of 13.5/9.8 Kb, representing 3.4/4.8-fold genome
576 coverage, for IR0F and IR13 lines respectively. Reads were mapped on the AaegL5 reference genome
577 using Winnowmap (Jain et al., 2022) and alignments were visualised using IGV (Robinson et al.,
578 2011). Finally, de novo genomes of the IR0F and IR13 lines were assembled using both Illumina short
579 reads and oxford nanopore long reads using MaSuRCA (Zimin et al., 2013). This de novo assembly
580 resulted into 17346/ 13160 contigs, with a median size of 40/55 kb for each line respectively.
581 Transposable elements were identified using BLAST against the RepBase library (10/12/2021
582 version).
583

584 *Quantification of the P450 duplication*

585 The detection of the P450 duplication was achieved through the quantification of *CYP6BB2* copy
586 number by digital droplet PCR (ddPCR). Genomic DNA was extracted from pools of mosquitoes using
587 the cetyltrimethylammonium bromide (CTAB) method (Collins et al 1987), resuspended in nuclease-
588 free water and quantified using Qubit DNA Broad Range assay (Qiagen). The duplex ddPCR
589 quantification assay was based on the co-amplification of two target genes each detected with
590 specific Taqman probes: the gene *CYP6BB2* (AAEL014893, Fam) was used to quantify the P450
591 duplication copy number while the gene *CYP4D39* (AAEL007808, Hex) always found as a single copy
592 in various *Ae. aegypti* lines was used as control for normalisation of gDNA quantities (Faucon et al.,
593 2015). Before amplification, gDNA samples were digested with XhoI for 15 min at 37°C directly within
594 the ddPCR reaction mixture. This reaction mixture was partitioned into up to 20,000 nanoliter-sized

droplets using the QX200 droplet generator (Bio-Rad) by mixing 70 µl of synthetic oil with 20 µl PCR mix. Then, 40µL of the partitioned reaction was then amplified for 40 cycles with an annealing temperature of 60°C (see **Supplementary file 8** for protocol details and primers/probes). After amplification, the number of positive and negative droplets was quantified for both Fam and Hex channels using the QX200 droplet reader (Bio-Rad) and the positive/negative ratio was used to estimate the initial gDNA concentration of each gene assuming a Poisson distribution. After normalisation for gDNA quantity, *CYP6BB2* copy number were expressed as mean copy number (± 95% CI).

Quantification of the Ile1011Met kdr mutation frequency

The frequency of the Ile1011Met kdr mutation was quantified on pools of mosquitoes using ddPCR. Genomic DNA was extracted as described above and digested with XhoI for 15 min at 37°C before partitioning. The duplex TaqMan reaction mixture contained two amplification primers together with two Taqman probes labelled with Fam and Hex fluorophores corresponding to the Met and Iso alleles respectively (see **Supplementary file 8** for protocol and primer/probes details). The duplex reaction mixture was emulsioned as described above and amplified for 40 cycles with an annealing temperature of 59°C. After droplet reading, the positive/negative ratio obtained for each channel was visualised as a scatterplot and was used to estimate the frequency of each allele assuming a Poisson distribution with 95% CI.

Aknowledgments

We thank the Institut Pasteur de La Guyane for providing the isofemale lines IR03 and IR13. We also thank Dr. Ademir Jesus Martins from the Fundación Oswaldo Cruz for a critical reading of the manuscript.

Conflict of interest disclosure

The authors declare that they comply with the PCI rule of having no financial conflicts of interest in relation to the content of the article.

Authors's contributions

JMB and JPD designed the study. TB, CH, JG, JC, MK, LN, TG, FL and JT performed experiments and analysed data. JF, FB, JV, JMB and JPD supervised data analysis. ID provided biological materials and data. JMB, JF and JPD acquired the funding. TB, JMB and JPD wrote and revised the paper.

Data availability

RNA-seq data have been deposited at EBI short read archive (SRA) under accession number E-MTAB-13325. DNA-seq short and long reads have been deposited at EBI short read archive (SRA) under accession number E-MTAB-13310.

Ethical aspects

Mice were kept in the animal facility of the Biology department of the University of Grenoble-Alpes, approved by the French Ministry of Animal Welfare (agreement no. B 38 421 10 001) and used in accordance with the laws of the European Union (directive 2010/63/EU). The use of animals for this study was approved by the ComEth Grenoble-C2EA-12 ethics committee mandated by the French Ministry of Higher Education and Research (MENESR). The study was conducted in accordance with the ARRIVE guidelines.

Funding

This study was partially supported by the European Union's Horizon 2020 research and innovation program under *ZIKAlliance* [grant agreement no. 734548]. This work was also supported by H2020 Research Infrastructures *Infravec2* [grant agreement no. 731060]. MK was supported a STMS fellowship funded by European Union's Horizon 2020 research and innovation under the *AIM COST action* [grant agreement no. CA17108]. The funders had no role in study design, data collection and interpretation, or decision to submit the work for publication.

Supplementary materials

Supplementary file 1 (.tiff image). Bioassays data from F1 and F2 offspring used to investigate the mode of inheritance of the resistance phenotype. Top: Controlled crosses used to generate F1 and F2 individuals used for bioasays. Bottom: Comparative mortality data obtained from the Bora-Bora and IR0F lines together with the F1 and F2 progeny of each cross in males and females. Deltamethrin exposure conditions were 0.03% deltamethrin for 30 min for females and 0.015% deltamethrin for 25 min for males to account for their inherent lower insecticide tolerance. Mortality rates are indicated as mean ± SD. Distinct letters indicate significantly distinct means (Kruskal-Wallis test followed by post hoc pairwise Wilcoxon test with Bonferroni-Holm correction, N=5, $p \leq 0.05$).

Supplementary file 2 (.xlsx file). RNA-seq and CNV data sets. All protein coding genes showing a significant differential transcription (sheet 'RNA-seq') or a significant differential exonic coverage (sheet 'CNV') are shown. See methods for filtering conditions and thresholds. Gene descriptions beginning with a # were manually inferred from Blast X result.

Supplementary File 3 (.tiff image). Genomic architecture of the *kdr* locus in the IR0F resistant line. On chromosome 3, the 3' part of the VGSC gene, including the 21 last exons, is duplicated. Black bars indicate the position of the coding exons. The duplication is 125 Kb long, and is imperfect: the two copies, R and R' mostly differing in their intronic sequences. The duplication breakpoints, left (LB) and right (RB) are located at 315,905,811 bp and 316,030,250 bp on the reference genome AaegL5. The 1011Met codon is located on the upstream copy (R) and followed by a B type intron. The 1011Ile codon is on the downstream copy and followed by an A type intron (Martins et al, 2013). RNA-seq data supported the sole expression of the 1011Met allele.

Supplementary file 4 (.xlsx file). Long reads overlapping the P450 duplication breakpoints.

Supplementary file 5 (.docx file). Data supporting the identification of the transposable elements flanking the P450 duplication.

Supplementary file 6 (.docx file). RNA interference experiment. This document includes detailed results and methods.

Supplementary file 7 (.tiff image). Proposed evolutionary steps leading to the observed duplication architecture. Theoretical structures and those inferred from short and long reads data are indicated. The hAt-like and PiggyBac-like transposons are shown in purple and green respectively. Transposition events are shown as dashed lines. The second hAt-like transposition event would have created an incomplete copy of the hAT transposon, either directly or through a posterior deletion. Recombination events are shown as blue crossed lines. Stars indicates junctions that were confirmed by short reads data.

Supplementary File 8 (.docx file). Digital droplet PCR assays used to quantify the P450 duplication and the frequency of the Ile1011Met kdr mutation. This document provides all technical details related these ddPCR assays including amplification primers, TaqMan probes, PCR conditions and data interpretation.

References

Achee, N. L., Grieco, J. P., Vatandoost, H., Seixas, G., Pinto, J., Ching-Ng, L., Martins, A. J., Juntarajumnong, W., Corbel, V., Gouagna, C., David, J.-P., Logan, J. G., Orsborne, J., Marois, E., Devine, G. J., & Vontas, J. (2019). Alternative strategies for mosquito-borne arbovirus control. *PLoS Negl Trop Dis*, *13*(1). https://doi.org/10.1371/journal.pntd.0006822

Anders, S., & Huber, W. (2010). Differential expression analysis for sequence count data. *Genome Biology*, *11*(10), R106. https://doi.org/10.1186/gb-2010-11-10-r106

Baker, M. D., Read, L. R., Beatty, B. G., & Ng, P. (1996). Requirements for Ectopic Homologous Recombination in Mammalian Somatic Cells. *Molecular and Cellular Biology*, *16*(12), 7122–7132. https://doi.org/10.1128/MCB.16.12.7122

Bariami, V., Jones, C. M., Poupardin, R., Vontas, J., & Ranson, H. (2012). Gene Amplification, ABC Transporters and Cytochrome P450s: Unraveling the Molecular Basis of Pyrethroid Resistance in the Dengue Vector, Aedes aegypti. *PLoS Negl Trop Dis*, *6*(6). https://doi.org/10.1371/journal.pntd.0001692

Bass, C., & Field, L. M. (2011). Gene amplification and insecticide resistance. *Pest Management Science*, *67*(8), 886–890. https://doi.org/10.1002/ps.2189

Benjamini, Y., & Hochberg, Y. (1995). Controlling the False Discovery Rate: A Practical and Powerful Approach to Multiple Testing. *J Royal Stat Soc B*, *57*, 289–300. https://doi.org/10.1111/j.2517-6161.1995.tb02031.x

Brengues, C., Hawkes, N. J., Chandre, F., McCarroll, L., Duchon, S., Guillet, P., Manguin, S., Morgan, J. C., & Hemingway, J. (2003). Pyrethroid and DDT cross-resistance in *Aedes aegypti* is correlated with novel mutations in the voltage-gated sodium channel gene. *Med Vet Entomol*, *17*(1), 87–94. https://doi.org/DOI: 10.1046/j.1365-2915.2003.00412.x

Brito, L. P., Carrara, L., Freitas, R. M. D., Lima, J. B. P., & Martins, A. J. (2018). Levels of Resistance to Pyrethroid among Distinct *kdr* Alleles in *Aedes aegypti* Laboratory Lines and Frequency of *kdr* Alleles in 27 Natural Populations from Rio de Janeiro, Brazil. *BioMed Research International*, *2018*, 1–10. https://doi.org/10.1155/2018/2410819

Brown, J. E., Evans, B. R., Zheng, W., Obas, V., Barrera-Martinez, L., Egizi, A., Zhao, H., Caccone, A., & Powell, J. R. (2014). Human impacts have shaped historical and recent evolution in *Aedes aegypti*, the dengue and yellow fever mosquito. *Evolution*, *68*(2), 514–525. https://doi.org/10.1111/evo.12281

Carvalho, V. L., & Long, M. T. (2021). Perspectives on New Vaccines against Arboviruses Using Insect-Specific Viruses as Platforms. *Vaccines*, *9*(3), 263. https://doi.org/10.3390/vaccines9030263

Cattel, J., Faucon, F., Le Peron, B., Sherpa, S., Monchal, M., Grillet, L., Gaude, T., Laporte, F., Dusfour, I., Reynaud, S., & David, J. P. (2020). Combining genetic crosses and pool targeted DNA-seq for untangling genomic variations associated with resistance to multiple insecticides in the mosquito Aedes aegypti. *Evolutionary Applications*, 303–317. https://doi.org/10.1111/eva.12867

Cattel, J., Haberkorn, C., Laporte, F., Gaude, T., Cumer, T., Renaud, J., Sutherland, I. W., Hertz, J. C., Bonneville, J., Arnaud, V., Fustec, B., Boyer, S., Marcombe, S., & David, J. (2021). A genomic amplification affecting a carboxylesterase gene cluster confers organophosphate resistance in the mosquito *Aedes aegypti*: From genomic characterization to high-throughput field detection. *Evolutionary Applications*, *14*(4), 1009–1022. https://doi.org/10.1111/eva.13177

Corbel, V., & N'Guessan, R. (2013). Distribution, Mechanisms, Impact and Management of Insecticide Resistance in Malaria Vectors: A Pragmatic Review, Anopheles mosquitoes -. *New insights into malaria vectors*. https://doi.org/10.5772/56117

David, J. P., Ismail, H. M., Chandor-Proust, A., & Paine, M. J. I. (2013). Role of cytochrome P450s in insecticide resistance: Impact on the control of mosquito-borne diseases and use of insecticides on Earth. *Philosophical Transactions of the Royal Society B-Biological Sciences*, *368*(1612). https://doi.org/10.1098/rstb.2012.0429

Djogbenou, L., Labbe, P., Chandre, F., Pasteur, N., & Weill, M. (2009). Ace-1 duplication in Anopheles gambiae: A challenge for malaria control. *Malar J*, *8*, 70. https://doi.org/10.1186/1475-2875-8-70

Dusfour, I., Thalmensy, V., Gaborit, P., Issaly, J., Carinci, R., & Girod, R. (2011). Multiple insecticide resistance in *Aedes aegypti* (Diptera: Culicidae) populations compromises the effectiveness of dengue vector control in French Guiana. *Mem Inst Oswaldo Cruz*, *106*(3), 346–352. https://doi.org/DOI: 10.1590/s0074-02762011000300015

Dusfour, I., Vontas, J., David, J. P., Weetman, D., Fonseca, D. M., Raghavendra, K., Corbel, V., Coulibaly, M., Martins, A. J., & Chandre, F. (2019). Management of insecticide resistance in the major Aedes vectors of arboviruses: Advances and challenges. *Plos Neg Trop Dis*, *13*(10), e0007615. https://doi.org/10.1371/journal.pntd.0007615

Dusfour, I., Zorrilla, P., Guidez, A., Issaly, J., Girod, R., Guillaumot, L., Robello, C., & Strode, C. (2015). Deltamethrin Resistance Mechanisms in Aedes aegypti Populations from Three French Overseas Territories Worldwide. *PLoS Negl Trop Dis*, *9*(11), e0004226. https://doi.org/10.1371/journal.pntd.0004226

Epelboin, Y., Wang, L., Giai Gianetto, Q., Choumet, V., Gaborit, P., Issaly, J., Guidez, A., Douché, T., Chaze, T., Matondo, M., & Dusfour, I. (2021). CYP450 core involvement in multiple resistance strains of Aedes aegypti from French Guiana highlighted by proteomics, molecular and biochemical studies. *PLOS ONE*, *16*(1), e0243992. https://doi.org/10.1371/journal.pone.0243992

Faucon, F., Dusfour, I., Gaude, T., Navratil, V., Boyer, F., Chandre, F., Sirisopa, P., Thanispong, K., Juntarajumnong, W., Poupardin, R., Chareonviriyaphap, T., Girod, R., Corbel, V., Reynaud, S., & David, J. P. (2015). Identifying genomic changes associated with insecticide resistance in the dengue mosquito Aedes aegypti by deep targeted sequencing. *Genome research*, *25*(9), 1347–1359. https://doi.org/10.1101/gr.189225.115

Faucon, F., Gaude, T., Dusfour, I., Navratil, V., Corbel, V., Juntarajumnong, W., Girod, R., Poupardin, R., Boyer, F., Reynaud, S., & David, J. P. (2017). In the hunt for genomic markers of metabolic resistance to pyrethroids in the mosquito *Aedes aegypti*: An integrated next-generation sequencing approach. *PLoS Negl Trop Dis*, *11*(4), e0005526. https://doi.org/10.1371/journal.pntd.0005526

Feyereisen, R., Dermauw, W., & Van Leeuwen, T. (2015). Genotype to phenotype, the molecular and physiological dimensions of resistance in arthropods. *Pesticide Biochemistry and Physiology*, *121*, 61–77. https://doi.org/10.1016/j.pestbp.2015.01.004

Ffrench-Constant, R. H., Daborn, P. J., & Le Goff, G. (2004). The genetics and genomics of insecticide resistance. *Trends Genet*, *20*(3), 163–170. https://doi.org/10.1016/j.tig.2004.01.003

Fontaine, A., Filipović, I., Fansiri, T., Hoffmann, A. A., Cheng, C., Kirkpatrick, M., Rašić, G., & Lambrechts, L. (2017). Extensive Genetic Differentiation between Homomorphic Sex Chromosomes in the Mosquito Vector, Aedes aegypti. *Genome Biology and Evolution*, *9*(9), 2322–2335. https://doi.org/10.1093/gbe/evx171

Garg, H., Mehmetoglu-Gurbuz, T., & Joshi, A. (2020). Virus Like Particles (VLP) as multivalent vaccine candidate against Chikungunya, Japanese Encephalitis, Yellow Fever and Zika Virus. *Scientific Reports*, *10*(1), 4017. https://doi.org/10.1038/s41598-020-61103-1

Goindin, D., Delannay, C., Gelasse, A., Ramdini, C., Gaude, T., Faucon, F., David, J. P., Gustave, J., Vega-Rua, A., & Fouque, F. (2017). Levels of insecticide resistance to deltamethrin, malathion, and temephos, and associated mechanisms in Aedes aegypti mosquitoes from the Guadeloupe and Saint Martin islands (French West Indies). *Infect Dis Poverty*, *6*(1), 38. https://doi.org/10.1186/s40249-017-0254-x

Haddi, K., Tome, H. V. V., Du, Y., Valbon, W. R., Nomura, Y., Martins, G. F., Dong, K., & Oliveira, E. E. (2017). Detection of a new pyrethroid resistance mutation (V410L) in the sodium channel of *Aedes aegypti*: A potential challenge for mosquito control. *Scientific Reports*, *7*, 46549. https://doi.org/10.1038/srep46549

Hawkins, N. J., Bass, C., Dixon, A., & Neve, P. (2018). The evolutionary origins of pesticide resistance. *Biol Rev Camb Philos Soc*. https://doi.org/10.1111/brv.12440

Hemingway, J., Hawkes, N. J., McCarroll, L., & Ranson, H. (2004). The molecular basis of insecticide resistance in mosquitoes. *Insect Biochemistry and Molecular Biology*, *34*(7), 653–665. https://doi.org/10.1016/j.ibmb.2004.03.018

Hendry, A. P., Farrugia, T. J., & Kinnison, M. T. (2008). Human influences on rates of phenotypic change in wild animal populations. *Molecular Ecology*, *17*(1), 20–29. https://doi.org/10.1111/j.1365-294X.2007.03428.x

Hendry, A. P., Gotanda, K. M., & Svensson, E. I. (2017). Human influences on evolution, and the ecological and societal consequences. *Philos Trans R Soc Lond B Biol Sci*, *372*(1712). https://doi.org/10.1098/rstb.2016.0028

Hirata, K., Komagata, O., Itokawa, K., Yamamoto, A., Tomita, T., & Kasai, S. (2014). A single crossing-over event in voltage-sensitive Na+ channel genes may cause critical failure of dengue mosquito control by insecticides. *PLoS Negl Trop Dis*, *8*(8), e3085. https://doi.org/10.1371/journal.pntd.0003085

Jain, C., Rhie, A., Hansen, N. F., Koren, S., & Phillippy, A. M. (2022). Long-read mapping to repetitive reference sequences using Winnowmap2. *Nature Methods*, *19*(6), 705–710. https://doi.org/10.1038/s41592-022-01457-8

Kasai, S., Itokawa, K., Uemura, N., Takaoka, A., Furutani, S., Maekawa, Y., Kobayashi, D., Imanishi-Kobayashi, N., Amoa-Bosompem, M., Murota, K., Higa, Y., Kawada, H., Minakawa, N., Cuong, T. C., Yen, N. T., Phong, T. V., Keo, S., Kang, K., Miura, K., … Komagata, O. (2022). Discovery of super–insecticide-resistant dengue mosquitoes in Asia: Threats of concomitant knockdown resistance mutations. *Science Advances*, *8*(51), eabq7345. https://doi.org/10.1126/sciadv.abq7345

Kasai, S., Komagata, O., Itokawa, K., Shono, T., Ng, L. C., Kobayashi, M., & Tomita, T. (2014). Mechanisms of pyrethroid resistance in the dengue mosquito vector, Aedes aegypti: Target site insensitivity, penetration, and metabolism. *PLoS Negl Trop Dis*, *8*(6), e2948. https://doi.org/10.1371/journal.pntd.0002948

Kondrashov, F. A. (2012). Gene duplication as a mechanism of genomic adaptation to a changing environment. *Proceedings. Biological Sciences / The Royal Society*, *279*(1749), 5048–5057. https://doi.org/10.1098/rspb.2012.1108

Kraemer, M. U., Sinka, M. E., Duda, K. A., Mylne, A. Q., Shearer, F. M., Barker, C. M., Moore, C. G., Carvalho, R. G., Coelho, G. E., Van Bortel, W., Hendrickx, G., Schaffner, F., Elyazar, I. R., Teng, H.-J., Brady, O. J., Messina, J. P., Pigott, D. M., Scott, T. W., Smith, D. L., … Hay, S. I. (2015). The global distribution of the arbovirus vectors Aedes aegypti and Ae. Albopictus. *eLife*, *4*, e08347. https://doi.org/10.7554/eLife.08347

Labbe, P., Berthomieu, A., Berticat, C., Alout, H., Raymond, M., Lenormand, T., & Weill, M. (2007). Independent duplications of the acetylcholinesterase gene conferring insecticide resistance in the

822 mosquito Culex pipiens. *Mol Biol Evol*, *24*(4), 1056–1067.
823 https://doi.org/10.1093/molbev/msm025

824 Li, X. C., Schuler, M. A., & Berenbaum, M. R. (2007). Molecular mechanisms of metabolic resistance
825 to synthetic and natural xenobiotics. *Annual Review of Entomology*, *52*, 231–253.
826 https://doi.org/10.1146/annurev.ento.51.110104.151104

827 Liu, N. (2015). Insecticide Resistance in Mosquitoes: Impact, Mechanisms, and Research Directions.
828 *Annual Review of Entomology*, *60*(1), 537–559. https://doi.org/10.1146/annurev-ento-010814-
829 020828

830 Lounibos, L. P. (2002). Invasions by insect vectors of human disease. *Annu Rev Entomol*, *47*, 233–266.
831 https://doi.org/10.1146/annurev.ento.47.091201.145206

832 Marcombe, S., Carron, A., Darriet, F., Etienne, M., Agnew, P., Tolosa, M., Yp-Tcha, M. M., Lagneau, C.,
833 Yebakima, A., & Corbel, V. (2009). Reduced efficacy of pyrethroid space sprays for dengue control
834 in an area of Martinique with pyrethroid resistance. *Am J Trop Med Hyg*, *80*(5), 745–751.
835 https://doi.org/10.4269/ajtmh.2009.80.745

836 Marcombe, S., Darriet, F., Tolosa, M., Agnew, P., Duchon, S., Etienne, M., Yp Tcha, M. M., Chandre, F.,
837 Corbel, V., & Yebakima, A. (2011). Pyrethroid resistance reduces the efficacy of space sprays for
838 dengue control on the island of Martinique (Caribbean). *PLoS Negl Trop Dis*, *5*(6), e1202.
839 https://doi.org/10.1371/journal.pntd.0001202

840 Marcombe, S., Fustec, B., Cattel, J., Chonephetsarath, S., Thammavong, P., Phommavanh, N., David,
841 J.-P., Corbel, V., Sutherland, I. W., Hertz, J. C., & Brey, P. T. (2019). Distribution of insecticide
842 resistance and mechanisms involved in the arbovirus vector Aedes aegypti in Laos and implication
843 for vector control. *PLOS Neglected Tropical Diseases*, *13*(12), e0007852.
844 https://doi.org/10.1371/journal.pntd.0007852

845 Marcombe, S., Poupardin, R., Darriet, F., Reynaud, S., Bonnet, J., Strode, C., Brengues, C., Yebakima,
846 A., Ranson, H., Corbel, V., & David, J.-P. (2009). Exploring the molecular basis of insecticide
847 resistance in the dengue vector Aedes aegypti: A case study in Martinique Island (French West
848 Indies). *BMC Genomics*, *10*. https://doi.org/494 10.1186/1471-2164-10-494

849 Martins, A. J., Brito, L. P., Linss, J. G., Rivas, G. B., Machado, R., Bruno, R. V., Lima, J. B., Valle, D., &
850 Peixoto, A. A. (2013). Evidence for gene duplication in the voltage-gated sodium channel gene of
851 Aedes aegypti. *Evolution, Medicine, and Public Health*, *2013*(1), 148–160.
852 https://doi.org/10.1093/emph/eot012

853 Martins, A. J., Lins, R. M., Linss, J. G., Peixoto, A. A., & Valle, D. (2009). Voltage-gated sodium channel
854 polymorphism and metabolic resistance in pyrethroid-resistant Aedes aegypti from Brazil. *Am J*
855 *Trop Med Hyg*, *81*(1), 108–115. https://doi.org/10.4269/ajtmh.2009.81.108

856 Melo Costa, M., Campos, K. B., Brito, L. P., Roux, E., Melo Rodovalho, C., Bellinato, D. F., Lima, J. B. P.,
857 & Martins, A. J. (2020). Kdr genotyping in Aedes aegypti from Brazil on a nation-wide scale from
858 2017 to 2018. *Scientific Reports*, *10*(1), 13267. https://doi.org/10.1038/s41598-020-70029-7

859 Moyes, C. L., Vontas, J., Martins, A. J., Ng, L. C., Koou, S. Y., Dusfour, I., Raghavendra, K., Pinto, J.,
860 Corbel, V., David, J. P., & Weetman, D. (2017). Contemporary status of insecticide resistance in
861 the major Aedes vectors of arboviruses infecting humans. *PLoS Negl Trop Dis*, *11*(7), e0005625.
862 https://doi.org/10.1371/journal.pntd.0005625

863 Nene, V., Wortman, J. R., Lawson, D., Haas, B., Kodira, C., Tu, Z. J., Loftus, B., Xi, Z., Megy, K.,
864 Grabherr, M., Ren, Q., Zdobnov, E. M., Lobo, N. F., Campbell, K. S., Brown, S. E., Bonaldo, M. F.,
865 Zhu, J., Sinkins, S. P., Hogenkamp, D. G., … Severson, D. W. (2007). Genome sequence of *Aedes*
866 *aegypti*, a major arbovirus vector. *Science*, *316*(5832), 1718–1723.
867 https://doi.org/10.1126/science.1138878

Orr, H. A. (2005). The genetic theory of adaptation: A brief history. *Nat Rev Genet*, *6*(2), 119–127. https://doi.org/10.1038/nrg1523

Palumbi, S. R. (2001). Humans as the world's greatest evolutionary force. *Science*, *293*(5536), 1786–1790. https://doi.org/10.1126/science.293.5536.1786

Reid, W. R., Thornton, A., Pridgeon, J. W., Becnel, J. J., Tang, F., Estep, A., Clark, G. G., Allan, S., & Liu, N. (2014). Transcriptional Analysis of Four Family 4 P450s in a Puerto Rico Strain of *Aedes aegypti* (Diptera: Culicidae) Compared With an Orlando Strain and Their Possible Functional Roles in Permethrin Resistance. *Journal of Medical Entomology*, *51*(3), 605–615. https://doi.org/10.1603/ME13228

Remnant, E. J., Good, R. T., Schmidt, J. M., Lumb, C., Robin, C., Daborn, P. J., & Batterham, P. (2013). Gene duplication in the major insecticide target site, *Rdl* , in *Drosophila melanogaster*. *Proceedings of the National Academy of Sciences*, *110*(36), 14705–14710. https://doi.org/10.1073/pnas.1311341110

Riaz, M. A., Chandor-Proust, A., Dauphin-Villemant, C., Poupardin, R., Jones, C. M., Strode, C., Regent-Kloeckner, M., David, J.-P., & Reynaud, S. (2013). Molecular mechanisms associated with increased tolerance to the neonicotinoid insecticide imidacloprid in the dengue vector Aedes aegypti. *Aquatic Toxicology*, *126*, 326–337. https://doi.org/10.1016/j.aquatox.2012.09.010

Rigby, L. M., Rašić, G., Peatey, C. L., Hugo, L. E., Beebe, N. W., & Devine, G. J. (2020). Identifying the fitness costs of a pyrethroid-resistant genotype in the major arboviral vector Aedes aegypti. *Parasites & Vectors*, *13*(1), 358. https://doi.org/10.1186/s13071-020-04238-4

Robinson, J. T., Thorvaldsdóttir, H., Winckler, W., Guttman, M., Lander, E. S., Getz, G., & Mesirov, J. P. (2011). Integrative genomics viewer. *Nature Biotechnology*, *29*(1), 24–26. https://doi.org/10.1038/nbt.1754

Saavedra-Rodriguez, K., Campbell, C. L., Lozano, S., Penilla-Navarro, P., Lopez-Solis, A., Solis-Santoyo, F., Rodriguez, A. D., Perera, R., & Black Iv, W. C. (2021). Permethrin resistance in Aedes aegypti: Genomic variants that confer knockdown resistance, recovery, and death. *PLOS Genetics*, *17*(6), e1009606. https://doi.org/10.1371/journal.pgen.1009606

Saavedra-Rodriguez, K., Suarez, A. F., Salas, I. F., Strode, C., Ranson, H., Hemingway, J., & Black, W. C. th. (2012). Transcription of detoxification genes after permethrin selection in the mosquito Aedes aegypti. *Insect Mol Biol*, *21*(1), 61–77. https://doi.org/10.1111/j.1365-2583.2011.01113.x

Saavedra-Rodriguez, K., Urdaneta-Marquez, L., Rajatileka, S., Moulton, M., Flores, A. E., Fernandez-Salas, I., Bisset, J., Rodriguez, M., McCall, P. J., Donnelly, M. J., Ranson, H., Hemingway, J., & Black, W. C. (2007). A mutation in the voltage-gated sodium channel gene associated with pyrethroid resistance in Latin American *Aedes aegypti*. *Insect Molecular Biology*, *16*(6), 785–798. https://doi.org/doi: 10.1111/j.1365-2583.2007.00774.x.

Schrider, D. R., Houle, D., Lynch, M., & Hahn, M. W. (2013). Rates and Genomic Consequences of Spontaneous Mutational Events in *Drosophila melanogaster*. *Genetics*, *194*(4), 937–954. https://doi.org/10.1534/genetics.113.151670

Seixas, G., Grigoraki, L., Weetman, D., Vicente, J. L., Silva, A. C., Pinto, J., Vontas, J., & Sousa, C. A. (2017). Insecticide resistance is mediated by multiple mechanisms in recently introduced Aedes aegypti from Madeira Island (Portugal). *PLoS Negl Trop Dis*, *11*(7), e0005799. https://doi.org/10.1371/journal.pntd.0005799

Silva, J. V. J., Lopes, T. R. R., Oliveira-Filho, E. F. D., Oliveira, R. A. S., Durães-Carvalho, R., & Gil, L. H. V. G. (2018). Current status, challenges and perspectives in the development of vaccines against yellow fever, dengue, Zika and chikungunya viruses. *Acta Tropica*, *182*, 257–263. https://doi.org/10.1016/j.actatropica.2018.03.009

Smith, L. B., Kasai, S., & Scott, J. G. (2016). Pyrethroid resistance in *Aedes aegypti* and *Aedes albopictus*: Important mosquito vectors of human diseases. *Pesticide Biochemistry and Physiology*, *133*, 1–12. https://doi.org/10.1016/j.pestbp.2016.03.005

Uemura, N., Furutani, S., Tomita, T., Itokawa, K., Komagata, O., & Kasai, S. (2023). Concomitant knockdown resistance allele, L982W + F1534C, in Aedes aegypti has the potential to impose fitness costs without selection pressure. *Pesticide Biochemistry and Physiology*, *193*, 105422. https://doi.org/10.1016/j.pestbp.2023.105422

Valle, D., Bellinato, D. F., Viana-Medeiros, P. F., Lima, J. B. P., & Martins Junior, A. D. J. (2019). Resistance to temephos and deltamethrin in Aedes aegypti from Brazil between 1985 and 2017. *Memórias Do Instituto Oswaldo Cruz*, *114*, e180544. https://doi.org/10.1590/0074-02760180544

Weetman, D., Djogbenou, L. S., & Lucas, E. (2018). Copy number variation (CNV) and insecticide resistance in mosquitoes: Evolving knowledge or an evolving problem? *Curr Opin Insect Sci*, *27*, 82–88. https://doi.org/10.1016/j.cois.2018.04.005

WHO. (2022). *Standard operating procedure for testing insecticide susceptibility of adult mosquitoes in WHO tube tests. SOP version: WHO Tube test/01/14.* World Health Organization. https://iris.who.int/bitstream/handle/10665/352316/9789240043831-eng.pdf?sequence=1

Yanola, J., Somboon, P., Walton, C., Nachaiwieng, W., Somwang, P., & Prapanthadara, L. A. (2011). High-throughput assays for detection of the F1534C mutation in the voltage-gated sodium channel gene in permethrin-resistant *Aedes aegypti* and the distribution of this mutation throughout Thailand. *Trop Med Int Health*, *16*(4), 501–509. https://doi.org/10.1111/j.1365-3156.2011.02725.x

Zimin, A. V., Marçais, G., Puiu, D., Roberts, M., Salzberg, S. L., & Yorke, J. A. (2013). The MaSuRCA genome assembler. *Bioinformatics*, *29*(21), 2669–2677. https://doi.org/10.1093/bioinformatics/btt476

Zoh, M. G., Gaude, T., Prud'homme, S. M., Riaz, M. A., David, J.-P., & Reynaud, S. (2021). Molecular bases of P450-mediated resistance to the neonicotinoid insecticide imidacloprid in the mosquito Ae. Aegypti. *Aquatic Toxicology*, *236*, 105860. https://doi.org/10.1016/j.aquatox.2021.105860